SERBIAN JOURNAL OF ELECTRICAL ENGINEERING
Vol. 17, No. 1, February 2020, 111-129

UDC: 546.26-162.544.227 **DOI: https://doi.org/10.2298/SJEE2001111V**

Analyses of the Surface Parameters in Polycrystalline Diamonds

Sandra Veljković[1], Vojislav Mitić[1,2], Vesna Paunović[1], Goran Lazović[3], Markus Mohr[4], Hans Fecht[4]

Abstract: There is a progressing interests for polycrystalline diamonds and they have been more extensively used recently. This area has been intensively researched due to the outstanding potential of this material, and this necessitated presenting some of the latest application related to engineering in this paper. A better insight of polycrystalline diamonds properties can be achieved by intensively researching the surface structure. Samples of nanocrystalline diamonds grown by the chemical vapor deposition method are analyzed and accordingly, the focus of the research was the surface parameters and their structure. It is observed that waviness and texture are unique for any direction, their values are almost the same for the chosen directions and they vary approximately from –0.2 nm to 0.4 nm. Analyses of the parameters allowed a more detailed insight into the morphology of the surfaces of polycrystalline films.

Keywords: Polycrystalline diamonds; Microelectronic devices; MEMS; Surface properties.

1 Introduction

Diamond is one of allotropic modifications of carbon and due to its specific structure, it has a very wide application [1]. Probably, it is most known for its use in jewelry, but it also has applications in medicine, in various industries for cutting, grinding, drilling and polishing [2]. Besides that, there is a very important use of diamonds in microelectromechanical systems (MEMS), microelectronics and in other areas. In addition, the possibility of using monocrystal and polycrystalline diamond materials for electronic devices is increasingly being explored [3 – 7].

[1]University of Niš, Faculty of Electronic Engineering, Aleksandra Medvedeva 14, 18000 Niš, Serbia; E-mails: sandra.veljkovic@elfak.rs; vmitic.d2480@gmail.com; vesna.paunovic@elfak.ni.ac.rs
[2]Institute of Technical Sciences, Knez Mihailova 35, 11000 Belgrade, Serbia; E-mail: vmitic.d2480@gmail.com
[3]University of Belgrade, Faculty of Mechanical Engineering, Kraljice Marije 16, 11000 Belgrade, Serbia; E-mail: goran.lazovic@gmail.com
[4]University of Ulm, Institute of Functional Nanosystems FNS, Albert-Einstein-Allee 45, 89081 Ulm, Germany; E-mails: markus.mohr@uni-ulm.de; hans.fecht@uni-ulm.de

However, natural diamonds are rear, expensive and it is hard to find them in proper sizes and shapes, which represents a limiting factor in their application. For that reason, the discovery that diamonds can be artificially synthesized was revolutionary. The first successful synthesis was achieved in the middle of the last century. The conditions in which diamonds are created in nature are artificially simulated: under high pressures (~GPa) and at high temperatures, which are about 1200°C. These parameters are used for the oldest technique for diamond synthesis, named high pressure high temperature (HPHT). Diamonds created by HPHT are very similar to natural diamonds. Although this technique is very effective, stone-like diamonds are not applicable in engineering. For that reason, a better solution is chemical vapor deposition (CVD) method, by which diamonds can be created as thin films for covering different surfaces and shapes. However, this CVD method is far from the thermodynamic equilibrium process, as can be seen in Fig. 1. The phase diagram is presented in this figure (pressure and temperature of carbon) and it shows the region of the stable phases of diamond, graphite and liquid carbon.

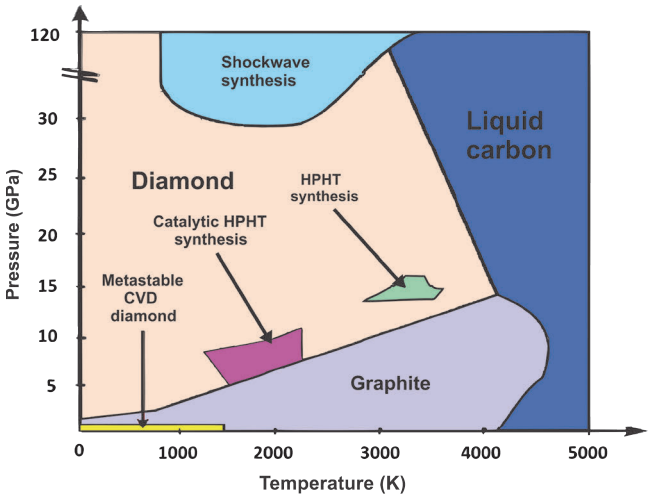

Fig. 1 – *Phase diagram shows stable carbon phases.*

In Fig. 1, areas of various growth methods are indicated, such as the shockwave synthesis, HPHT synthesis and catalytic HPHT synthesis, and finally, CVD diamond growth in the metastable region (far from the area of natural diamonds growth).

Characteristics and properties of natural diamonds are the result of their specific structure, which is presented in Fig. 2a. It shows a unit diamond cell where each carbon atom is linked to the four nearest neighbors. The bond is made by sp^3 hybridized orbitals with angles of 109.5° between all neighbor

bonds (Fig. 2b). Two intermediate surface-centered cubic lattices, which are shifted one of other one-quarter of its length can be seen in the diamond crystal structure. Each unit cell has eight atoms.

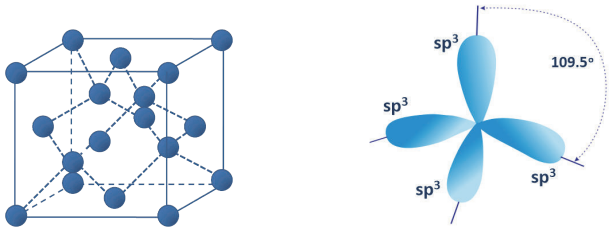

(a) (b)

Fig. 2 – (a) *Crystal structure of diamond;* (b) *sp^3- hybrid orbitals.*

Due to its structure, diamond is the hardest material on the Mohs scale with the value of 10; it has the highest melting temperature that is 3547 °C and the lowest molar entropy of 2.4 J mol^{-1} K^{-1}. Similarly, mechanical properties of diamonds are very interesting. Symmetrical tetrahedral structure and relatively short links between carbon atoms cause a very high value of the Young's modulus – 1050 GPa. Also, monocrystalline diamond has high fracture strength, about 2.8 GPa [8], that is by far the highest fracture strength value of all materials that are used for micro-mechanical purposes.

Despite great qualities of natural diamonds, it is not profitable to use them in mass production due to the high price and complex processing. For that reason, diamond synthesis was a significant discovery, as it became possible to apply diamond layers on different materials and shapes.

2 Application of Polycrystalline Diamonds

Diamonds obtained by the CVD technique can be microcrystalline diamonds (MCD) and their grain size order of magnitude is micrometric. The main characteristics of these layers are that they are very rough and have a very low resistance to fracture which limits their application. Further development and improving of the CVD technique, made it possible to control the size of grain. Different forms of diamonds have been developed (with smaller grains) like nanocrystalline diamond (NCD) and ultra-nanocrystalline diamond (UNCD). These diamond materials have different structures and usage, but, what is the most important, they have significantly better properties in terms of mechanical strength and tribological characteristics in relation to MCD.

The progress in development of the CVD method enabled control of the grain size, from micrometric to nanometric size. Grains, despite of their size, are always separated by non-diamond material such as graphite and C-H bonds with

sp^2 and sp^3 hybridized carbon [1]. For that reason, any variation in the grain size of crystal can lead to a major impact on the total amount of atoms which are in contact with grain boundaries. In that sense, depending on the microstructure, the properties can be determined, and consequently, the possible uses of these materials.

These novel materials are very interesting for application in MEMS, because of their mechanical and electrical properties. There is a requirement for the application of MEMS in sensitive and specific conditions [4].

Considering that polycrystalline diamonds perform well, their application in MEMS components is increasingly frequent. The advanced researches concern with how to replace MEMS components in sensors with nanoelectromechanical systems (NEMS). Replacing them would create a possibility to increase the resonant frequency and thus, the sensitivity of the sensor structure. NEMS structures can be made of different materials enabling optimization of individual properties such as hardness, low dissipation, compatibility with the work area, and easier production method and better integration [5].

Structural properties of the high conductivity UNCD were especially investigated in order to determine the origin of electrical conductivity. During researching, it was observed that a small amount of nano-graphite exists between diamond grains. The mechanism which is responsible for conductivity in UNCD is attributed to the effect of πsp^2 bounds at the grain boundaries. The connection between structural properties of sp^2 carbon bounds and specific conductivity is observed. Specific conductivity is firstly affected by structural properties of grain boundaries. Conductivity of thin films at room temperature can be explained by very low activation energies (meV), of sp^2 carbon bounds.

One of possible uses of polycrystalline diamonds is in radiofrequency (RF) MEMS resonators, and these materials were examined for this application [6].

Also, there has been an increased interest in the application of polycrystalline diamonds in sensors (piezo-resistant, temperature, gas and biosensors) due to their unique combination of properties [7, 9]. Among other properties, they are chemically inert, resistant to corrosion, they have flexible modification of the surface, but the most important is that they are not toxic for humans and animals.

Fig. 3a illustrates the diamond probe in certain formation steps, while Fig. 3b shows the final form.

The development of bioMEMS has also led to the development of new multifunctional probes that can record individual neural activities and detect extracellular transmitters (Fig. 4). It causes the development of a new generation of healthcare systems. Multifunctional integrated microsystems

contain single material MEMS (SMM). A surgically inserted probe was used to record the neural activity for the first time in vivo. The probe was inserted into the auditory cortex of the guinea pig brain.

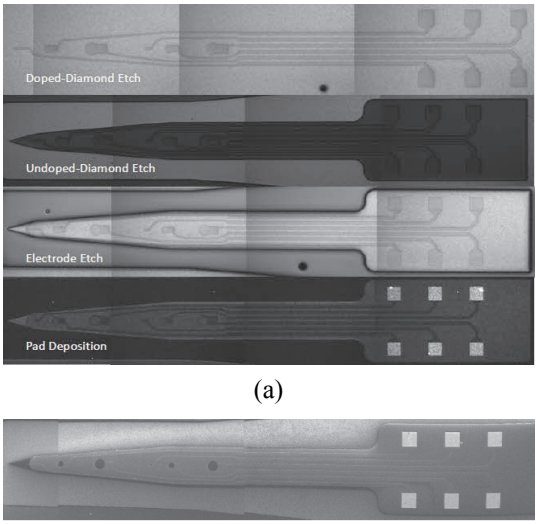

(a)

(b)

Fig. 3 – *Illustration of the diamond probe layout:*
(a) *in certain formation steps;* (b) *final appearance* [7].

A polycarbonate probe of micrometer or nanometer dimensions can detect both chemical and electrical signals with the same structure. The manufacturing of such a probe requires the use of six masks. The schematic of the probe in Fig. 5a shows the details of dimensions and, it can be seen that it is flexible and transparent (Figs. 5b and c). The probe shown has eight positions (which are highly doped) with diameters ranging from 2 μm to 150 μm [10].

Information on the development of electronic components such as resistors, capacitors, Schottky's diodes, p-n diodes, thyristors, which structures are based on diamond material, can be found in the literature.

Specifically, diamond materials exhibit attractive semiconductor properties (due to a wide band gap, high thermal conductivity and relatively high carrier velocity), which makes them very interesting for powerful, high-frequency and high-temperature microelectronic components that can operate in harsh environments (high temperatures and/or radiation). The development of transistor technology, based on these materials, was delayed, among other things, due to doping difficulty. The innovative approach of p-doping (formation of p-type semiconductor material) by hydrogenating the surface (H-

terminated diamond) led to promising results in the formation of MESFET (metal-semiconductor field-effect transistor) [11].

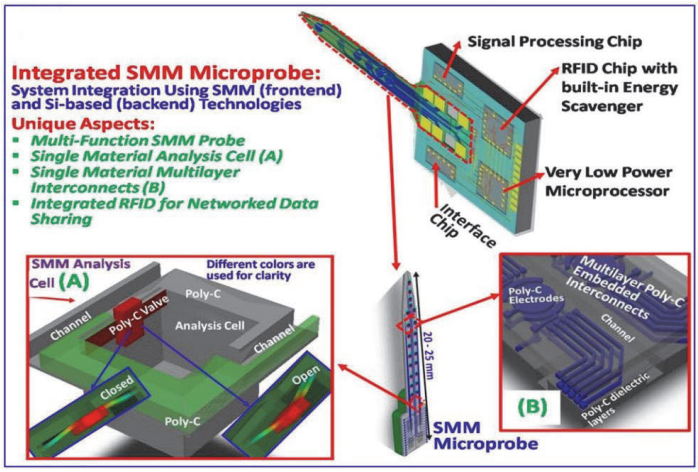

Fig. 4 – *Diagram of a multifunctional integrated microsystem for biosensors* [7].

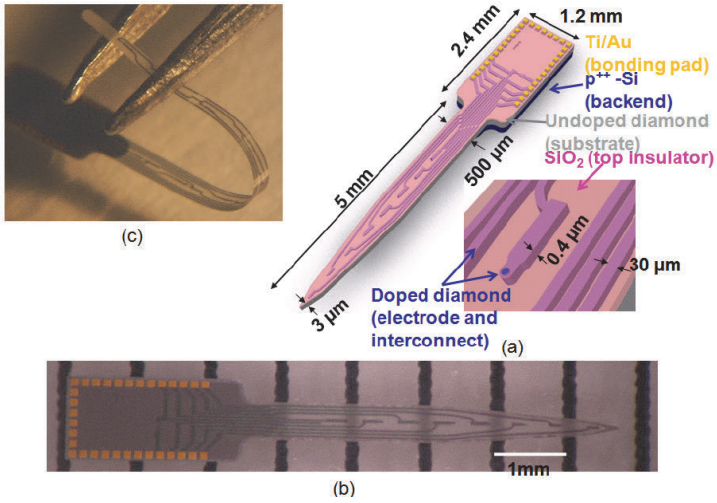

Fig. 5 – (a) *Schematic representation of the probe;* (b) *probe made;* (c) *background representation of the probe* [10].

Also, one of the serious technological problems was the growth of diamonds on the substrate. The result was mainly polycrystalline diamond layers and materials that were suitable for MEMS but not for electronic components. There was an encouraging result when the growth of

monocrystalline diamond material on iridium, which is suitable for electronic components, was successfully achieved [12].

Fig. 6 shows the structure of a diode which consists of an undoped 0.5 μm diamond layer, located between the metal (palladium-Pd) and doped diamond layer. The same figure also shows the current-voltage characteristic of this diode, where it can be observed that the breakdown voltage is 500 V. This diode has a high resistance in direct polarization [12].

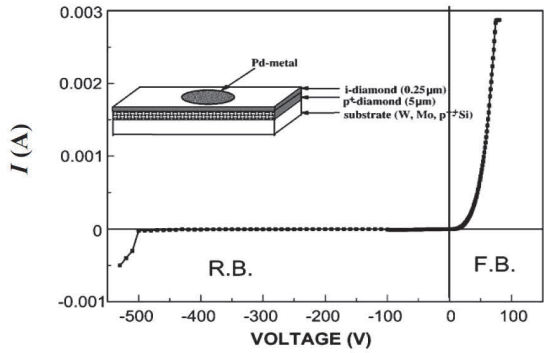

Fig. 6 – *Schematic representation of a diamond-tipped diode and its current-voltage characteristic* [12].

Such diodes have extremely high breakdown voltages compared to silicon or silicon carbide components, as can be seen in Fig. 7, where breakdown voltages are shown depending on the doping level (concentration of impurity) for silicon, silicon carbide and Schottky diamond diodes.

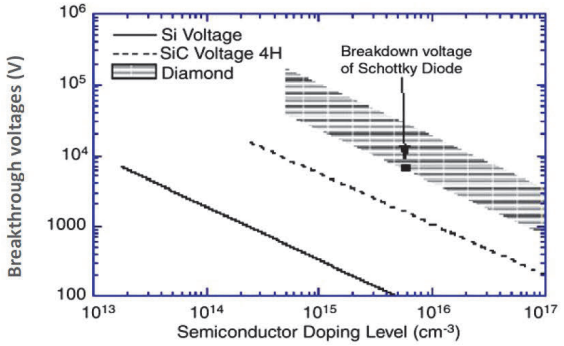

Fig. 7 – *Breakthrough voltages depending on the impurity concentration for Si, SiC, and diamond Schottky diodes* [12].

Fig. 8 shows a cross section of a MISFET (metal oxide semiconductor field-effect transistor) which gate length is 0.7 μm and its current-voltage

characteristics. The characteristics of this FET type structure are in the GHz range, so research of such structures is intensive. The conductive channel is located on the surface and is formed by hydrogenating the surface of the diamond material (H-terminated diamond). This channel is in fact a two-dimensional hole gas (2DHG), although the exact location (at or below the surface) is not completely known, nor is the nature of the acceptor, which has not yet been elucidated. Considering that the processes are associated to the surface, the knowledge of the surface properties is very important [12].

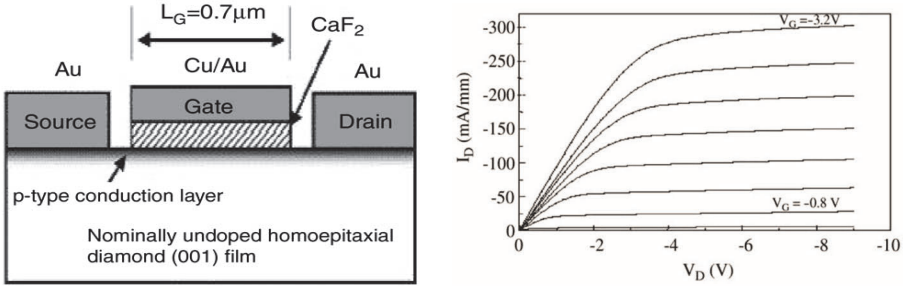

(a) (b)

Fig. 8 – (a) *Cross section of a MISFET whose gate length is* 0.7 μm; (b) *I–V characteristics* [12].

Also, the usage of polycrystalline diamonds in the mechanical industry is very frequent, and especially for cutting, drilling or treating materials which are very complicated for processing such as carbon fiber reinforced plastics, plastic foils with metal additives. The optical and thermal properties of microcrystalline diamonds with large grains are very useful for optical windows (for high-power laser window, vacuum windows, and microwave windows) or head spreaders.

The combination of the high wear-resistance and the low friction coefficient of smooth diamond surface make this material ideal for mechanical watch movements, where important parameters are reliability, lifetime and accuracy. The production of mechanical watches represents one of few traditional crafts standing opposite to ever-increasing automation and mass production, which are increasingly present. However, traditional materials such as steel, nickel and ruby which are used in traditional manufacturing, now can be replaced with silicon and synthetic diamonds. The main aim of watch manufacturers is to produce an oil-free watch mechanism, which explains the demand for materials with very good tribological properties [7, 13].

Therefore, it is imperative to continue examining the surface structure of diamond materials, as well as the parameters that characterize it, in order to establish a correlation with the material characteristics.

3 Experimental Procedure and Apparatus Setup

Knowledge of the structure of materials, on which their properties depend, can contribute to understanding not only the mechanical but also other properties of these materials. An electron microscope can be used very successfully for a detailed analysis of the material. Scanning electron microscope (SEM) is used for characterization and analysis of materials in in many areas, and its application is very important in the field of electronics. In the experiment, measuring was performed in the Laboratory for Electron Microscopy, University of Niš. Electron microscope of the type JEOL JSM 5300 with accompanying equipment for visualization, processing and acquisition of the obtained results was used.

Fig. 9 shows the test specimens of the appropriate size attached to the base by a conductive strip prepared for the analysis. These are the parts of three-inch wafers on which nanocrystalline diamond films were formed in a hot filament chamber at the Institute of Functional Nanosystems, University of Ulm.

In the used microscope, an accelerating voltage in the range of 0.5 kV to 30 kV is applied. The resolution of the microscope is 4.5 nm, and the magnification that can be achieved is from 10 to 200 000, although, in practice, the magnification cannot be more than 100 000. The spot that can be observed by this microscope is 80×40 mm. The samples have to be treated according to the prescribed procedure before an analysis.

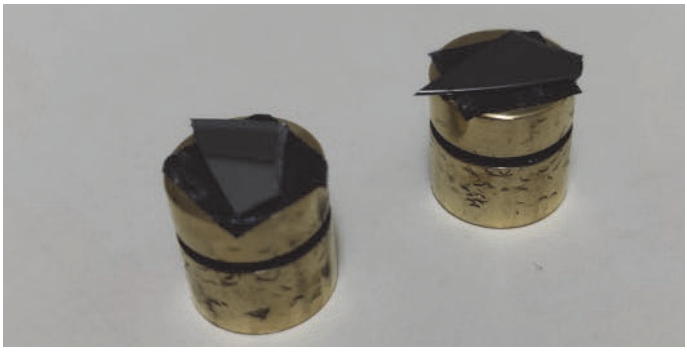

Fig. 9 – *Test specimens prepared for microscope analysis.*

The inside of the microscope chamber should not be manipulated without protective gloves. It should be verified that the sample is not in contact with any of the surrounding surfaces, and especially with the upper surface after carefully closing the chamber door.

The surface images of the sample obtained by applying a voltage of 30 000 V and at magnifications of 10 000 and 15 000 are shown in Fig. 10.

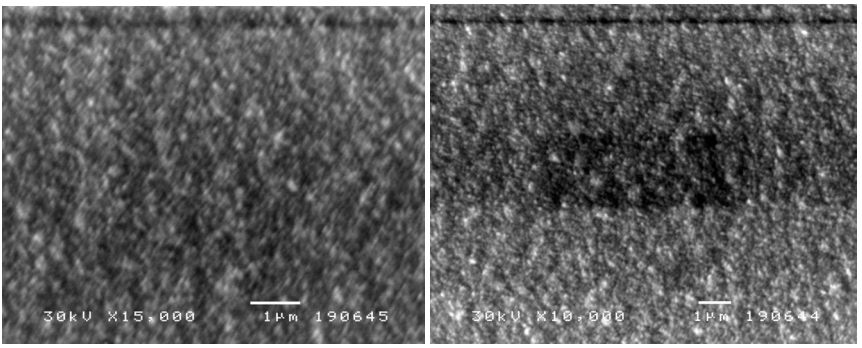

(a) (b)

Fig. 10 – *Images of the surfaces of the sample obtained by a voltage of* 30 000 V *and at a magnification of* (a) 15 000 *and* (b) 10 000.

In Fig. 11 is presented a 3D view of the polycrystalline diamond surface of the analyzed sample. Dimensions of the analyzed part of the surface are 4.4 μm and 4.5 μm, while the height of grains is in the range from 0 μm to 0.91 μm.

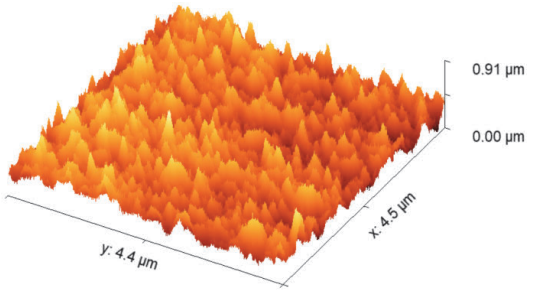

Fig. 11 – *3D view of polycrystalline diamond surface.*

4 Analysis of Polycrystalline Diamonds Surface

For further analysis standardized surface parameters [14] and one-dimensional texture parameters were evaluated separately.

The roughness r_j is defined as:

$$r_j = z_j - \overline{z}\,, \tag{1}$$

where z_j is pixel-centered vertices and $\overline{z}$ is the mean value of z.

First, the Roughness Average R_a, was determined, which represents the average deviation of the roughness profile of all points from the mean line, along the selected direction. This parameter can be calculated by:

$$R_a = \frac{1}{N}\sum_{j=1}^{N}\left| r_j \right| . \tag{2}$$

For the observed sample, Fig. 12 shows the roughness for the selected direction, which was used in determining the parameter R_a and the value of this parameter is 22.65 pm.

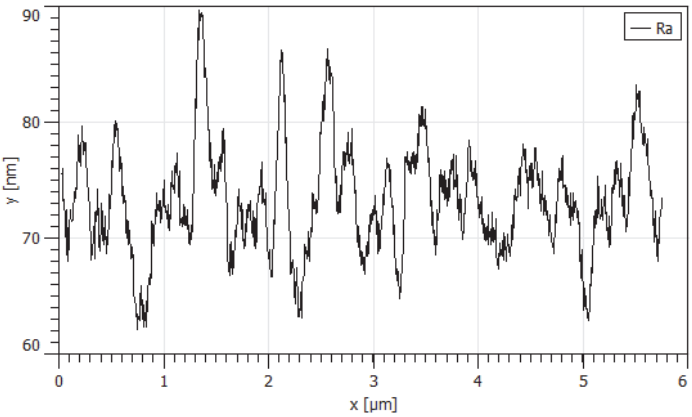

Fig. 12 – *Determination of parameter R_a - mean roughness value.*

Root Mean Square Roughness (RMS) R_q represents the average of the measured height deviations taken within the evaluation length and measured from the mean line in the selected direction:

$$R_q = \sqrt{\frac{1}{N}\sum_{j=1}^{N} r_j^2} , \tag{3}$$

where N is the number of samples along the assessment length.

For the observed sample, the determination of the RMS parameter for the selected direction is shown in Fig. 13 and the value of this parameter is 28.95 pm.

The Maximum Profile Valley Depth R_v or R_m was then determined. It can be calculated by:

$$R_V = \left| \min_{1<j<N} r_j \right| . \tag{4}$$

This parameter represents the deepest part of the profile (sample) in the observed direction and its value for the sample is 165.82 pm.

In the next step, the Maximum Profile Peak Height R_p is determined. It can be calculated by:

$$R_P = \left| \max_{1<j<N} r_j \right| . \tag{5}$$

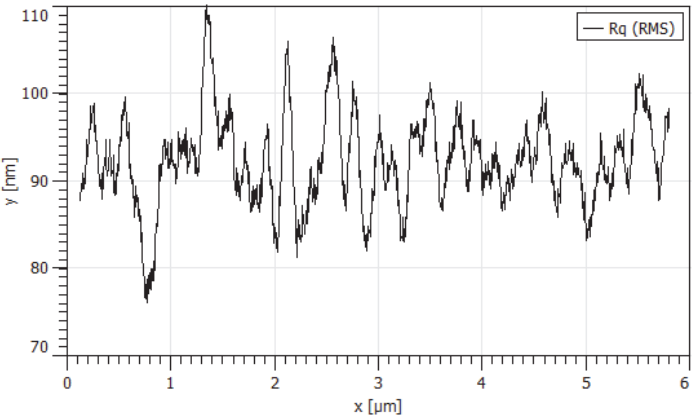

Fig. 13 – *Determination of parameter R_q - root of square root roughness.*

The parameter R_p represents the highest peak, in the observed direction, i.e. the highest part of the profile (sample) in the observed direction and its value for the sample is 123.13 pm.

The next parameter that is specified represents the Average Maximum Height of the Profile R_{tm}. This parameter represents the maximum mean value of profile roughness in the observed direction, and it can be calculated by the following formula.

$$R_{tm} = R_{vm} + R_{pm} . \tag{6}$$

It is determined by the difference between the highest and lowest peak values in a given direction and its value for the sample is 176.217 pm.

In the next step, the Average Maximum Profile Valley Depth – R_{vm} is determined and it can be calculated by:

$$R_{vm} = \frac{1}{m}\sum_{i=1}^{m} R_{vi} , \tag{7}$$

where R_{vi} is:

$$R_{vi} = \left|\min r_j\right| \text{ for } (i-1)\frac{N}{m} < j < i\frac{N}{m} . \tag{8}$$

The R_{vm} parameter is determined based on at least 5 peaks determined for different chosen directions and it represents the mean depth of the profile. Its value for the sample is 93.28 pm.

Finally, the Average Maximum Profile Peak Height – R_{pm} is determined, and it can be calculated by:

$$R_{pm} = \frac{1}{m}\sum_{i=1}^{m} R_{pi}\,, \tag{9}$$

where R_{pi} is:

$$R_{pi} = \left|\max r_j\right| \text{ for } (i-1)\frac{N}{m} < j < i\frac{N}{m}\,. \tag{10}$$

The R_{pm} parameter is determined based on at least 5 peaks determined for different chosen directions and it represents the mean height of the profile. Its value for the sample is 82.94 pm

After determining these parameters, the appropriate functions that allow a more detailed insight into the morphology of the surfaces of polycrystalline films were defined.

The ADF (Amplitude Distribution Function) for the selected direction was also simulated. It represents a probability function that further describes the sample surface, representing the probability that there is a certain height z at any position x, in a precisely defined direction, of the sample surface. The result obtained for the observed sample is shown in Fig. 14.

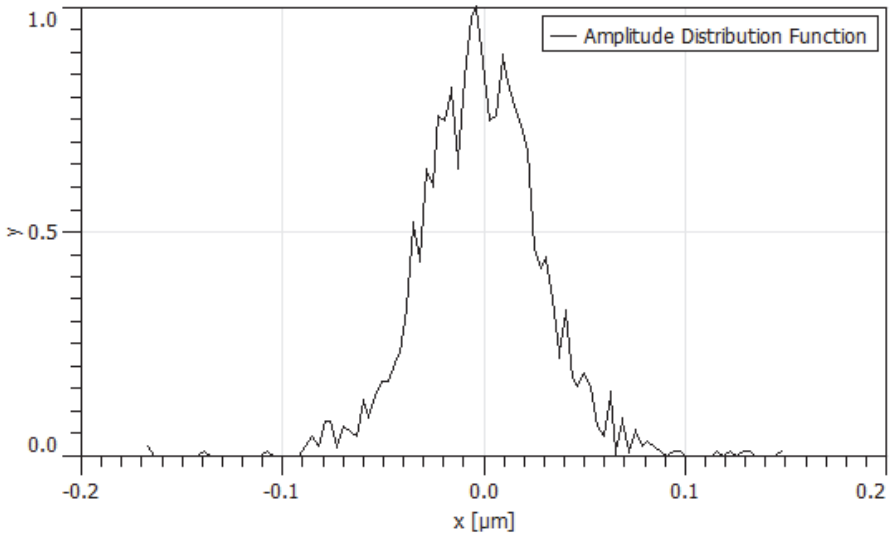

Fig. 14 – *ADF function - amplitude distribution function for selected direction.*

Then, the BRC (Bearing Ratio Curve) function, which is directly related to the ADF function, represents the corresponding cumulative probability function. It represents a certain integral of the ADF function, with the integration from the highest to the smallest value along the y direction of the ADF function. The BRC function of the analyzed sample is shown in Fig. 15.

Skewness is a parameter that describes the shape of ADF. Skewness is a simple measure of the asymmetry of ADF, or, equivalently, it measures the symmetry of the variation of a profile about its mean line which can be calculated by:

$$R_{sk} = \frac{1}{NR_q^3}\sum_{j=1}^{N} r_j^3 \,. \tag{11}$$

The value of this parameter R_{sk} for the sample is 0.03407.

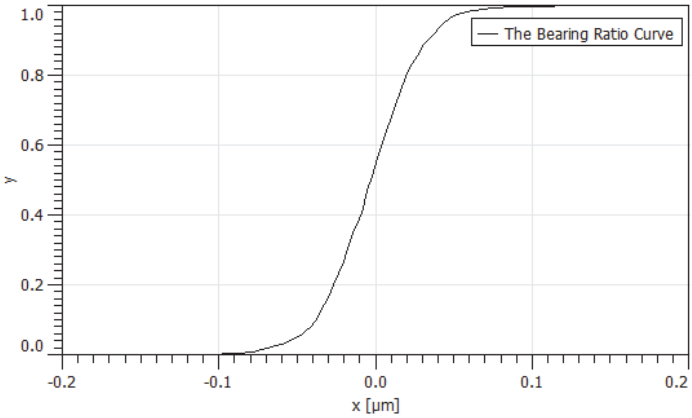

Fig. 15 – *BRC functions.*

Also, Minkowski functions can contribute to a more detailed understanding of the surface of polycrystalline diamonds. These functions are used to describe the standard geometric characteristics of a structure. The two-dimensional parameters, volume V, surface P and connectivity (Euler-Poincaré Characteristic) χ, which are used to describe them, are calculated using the following relations:

$$V = \frac{N_{white}}{N}, \quad S = \frac{N_{bound}}{N}, \quad \chi = \frac{C_{white} - C_{black}}{N}. \tag{12}$$

N represents the correct number of pixels, N_{white} is the number of "white" pixels, pixels that are above the limit value. Pixels below the cut-off value are called “black” pixels. The N_{bound} parameter represents the difference between “white” and “black” pixels. Lastly, C_{white} and C_{black} represent the number of continuous sets of “white” and “black” pixels, respectively. These parameters are presented as a function of parameter J, which is a parameter that represents the difference between values of “white” and “black” pixels. All parameters, $V(J)$, $S(J)$ and $\chi(J)$, are shown for the investigated sample are shown in Fig. 16.

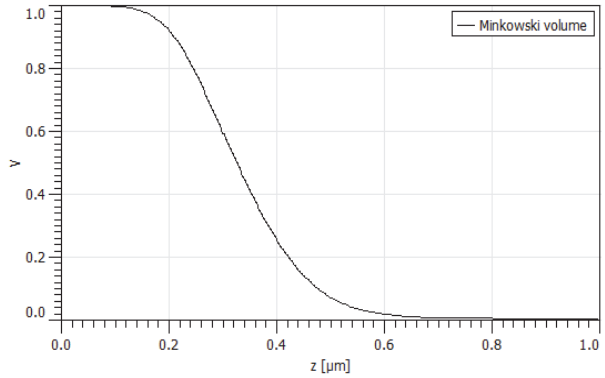

(a)

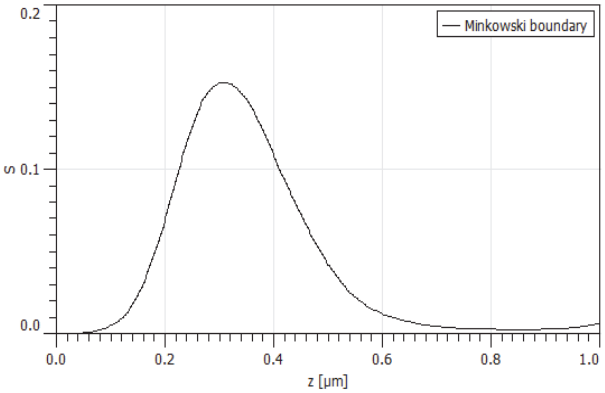

(b)

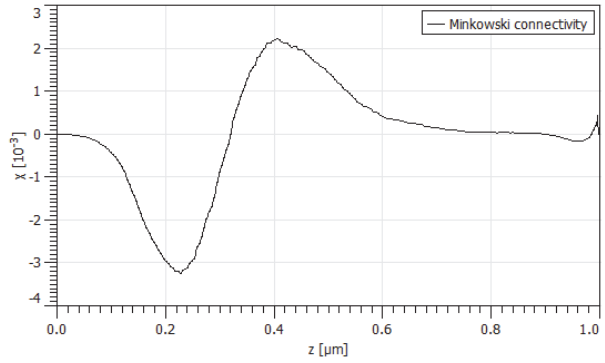

(c)

Fig. 16 – *Parameters of the Minkowski function for the sample:* (a) *volume V;* (b) *surface P, and* (c) *connectivity* χ.

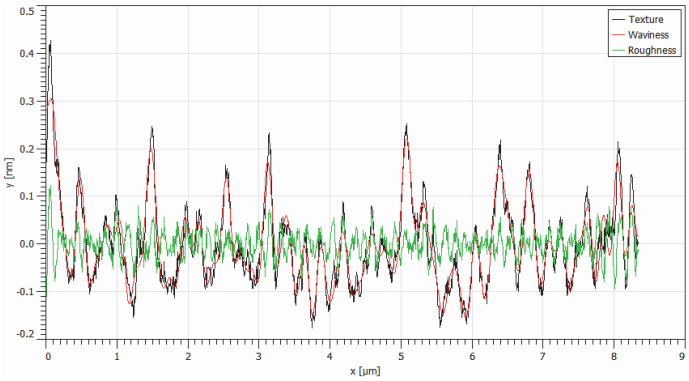

Fig. 17 – *Texture parameters of polycrystalline surface.*

In addition, in further analysis, texture parameters were analyzed. The one-dimensional texture parameter is divided into waviness, which represents the low-frequency component that participates in defining the surface, and the roughness, which represents the high-frequency component that participates in defining the surface, at the cut-off frequency. This frequency is defined in units of Nyquist frequency, that is the value of 1.00 corresponds to the Nyquist frequency. The mean r_j is assumed to be zero. The texture parameters, as well as the waviness and roughness, for a given direction, for the sample, are shown in Fig. 17.

It can be seen that the texture and waviness shapes are practically the same. The most pronounced peaks correspond to the highest parts of the grains for the chosen direction. Although, the waviness and texture are unique for any chosen direction, their values vary approximately from –0.2 nm to 0.4 nm for the chosen direction.

The analysis may need to determine the position of the grain (grown around the seed). In that sense the simulations were used to determine the local minimum, segmentation, and grain boundaries. Regarding that the problem of determining the position of the grain can be understood as a problem of finding the local maximum on the surface, the Voronoi diagram can contribute to the analysis of grain position. Namely, the Voronoi diagram is a partition of a plane into regions close to each of a given set of objects. In the simplest case, these objects are just a finite number of points in the plane (called seeds, sites, or generators). All points of a plane closer a specific seed than to any other, constitute a corresponding region for that seed. The name of these regions is Voronoi cells. The Lattice parameters, which are applied, can be used for estimation of the Voronoi diagram.

The final surface is constructed as a weighted sum of a subset of basic quantities derived from the Voronoi diagram. Border distance, Radial distance

and Segmented distance are some quantities which are available. The distance to the closest Voronoi cell border is the Border distance. The distance to the closest point of the set is the Radial distance. The distance to the closest Voronoi cell border is the Segmented distance, scaled in each cell segment so that the set point is at the same distance from all borders. Fig. 18a presents the sample, and Fig. 18b presents the Lattice parameters.

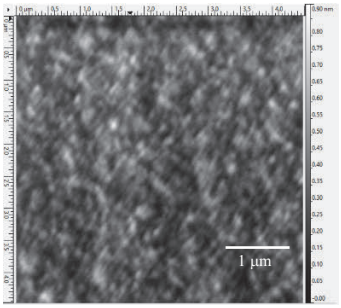

(a)

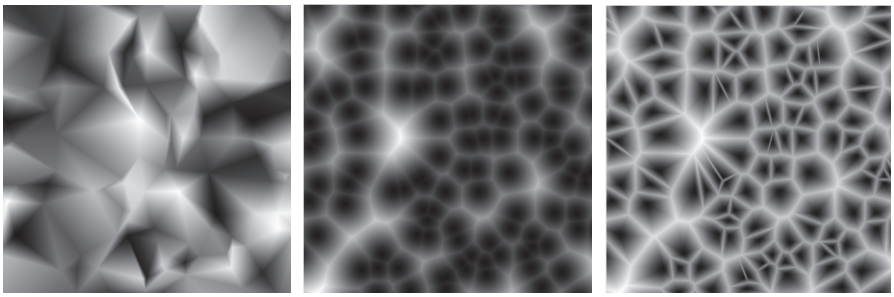

(b)

Fig. 18 – (a) *the sample;* (b) *Lattice parameters – border, radial and segmented distances.*

5 Conclusion

Outstanding electrical, thermal, mechanical and tribological properties have made it possible to apply polycrystalline diamonds in many areas, in industry, production of mechanical watches, medicine and especially for advanced electronics. Polycrystalline diamonds have a very important role in microelectronic and microelectromechanical systems as a material used for sensors and probes. It is necessary to be familiar with characteristics of polycrystalline diamonds in order to improve current applications and also, to develop new ones. Considering that intensive research over the past years showed that the properties of materials with nanometric dimensions are significantly different from those of bulk materials, a detailed analysis of

surface characteristics, which includes various parameters, is also very important.

In this paper an analysis of the polycrystalline diamond surface structure was performed. By using 2D analysis, here are presented R_a, R_q, R_t, R_v, R_p, R_{tm}, R_{vm}, R_{pm}. Analyzes of these parameters allowed a more detailed insight into the morphology of the surfaces of polycrystalline films. It was observed that for chosen direction, the texture feature is similar to the waviness. Although, waviness and texture are unique for any direction, their values are almost the same for the chosen directions and vary approximately from –0.2 nm to 0.4 nm. By varying growth parameters, it is possible to influence the properties of polycrystalline diamond films for specific applications. Also, in order to determine the position of the grains, in the paper are presented Lattice parameters – Border distance, Radial distance and Segmented distance.

Acknowledgment

These researches represent results which are a part of the project OI 172057, that is financially supported of Serbian Ministry of Education, Science and Technological Development. Also, this paper is realized in cooperation with the Institute of Functional Nanosystems, University of Ulm, in Germany and the Laboratory for Electron Microscopy, University of Niš.

6 References

[1] M. Wiora: Characterization of Nanocrystalline Diamond Coatings for Micro-Mechanical Applications, Ph. D. Dissertation, Ulm University, Ulm, Germany, 2013.

[2] Diamond Films Handbook, Edited by J. Asmussen and D. K. Reinhard, 1st edition, CRC Press, New York, Basel, 2002.

[3] S. Veljković, V. Mitić, V. Paunović, G. Lazović, M. Mohr, H. Fecht: Surface Properties of Polycrystalline Diamonds for Advanced Applications, Proceedings of the 6th International Conference on Electrical, Electronic and Computing Engineering (IcETRAN), Silver Lake, Serbia, June 2019, pp 652 – 656.

[4] Carbon-Based Nanomaterials and Hybrid Synthesis, Properties, and Commercial Applications, Edited by H. J. Fecht, K. Brühne and P. Gluche, 1st edition, Pan Stanford, Singapore, 2014.

[5] L. Sekaric, J. M. Parpia, H. G. Craighead: Nanomechanical Resonant Structures in Nanocrystalline Diamond, Applied Physics Letters, Vol. 81, No. 23, December 2002, pp. 4455 – 4457.

[6] N. Sepúlveda-Alancastro: Polycrystalline Diamond RF MEMS Resonator Technology and Characterization, Ph. D. Dissertation, Michigan State University, East Lansing, USA, 2005.

[7] M. W. Varney, D. M. Aslam, A. Janoudi, H.- Y. Chan, D. H. Wang: Polycrystalline-Diamond MEMS Biosensors Including Neural Microelectrode-Arrays, Biosensors, Vol. 1, No. 3, September 2011, pp. 118 – 133.

[8] Properties of Natural and Synthetic Diamond, Edited by J. E. Field, 1st edition, Academic Press, San Diego, London, 1992.

[9] S. Veljković, V. V. Mitić, V. Paunović, G. Lazović, M. Mohr, H. Fecht: Characteristics and Applications of Polycrystalline Diamonds, Proceedings of the IEEESTEC 11th Student Projects Conference, Niš, Serbia, November 2018, pp. 181 – 184. (In Serbian).

[10] H.- Y. Chan, D. M. Aslam, J. Wiler, B. Casey: A Novel Diamond Micro Probe for Neuro-Chemical and Electrical Recording in Neural Prosthesis, Journal of Microelectromechanical Systems, Vol. 18, No. 3, June 2009, pp. 511 – 521.

[11] V. Camarchia, F. Cappelluti, G. Ghione, E. Limiti, D. A. J. Moran, M. Pirola: An Overview on Recent Developments in RF and Microwave Power H-Terminated Diamond MESFET Technology, Proceedings of the International Workshop on Integrated Nonlinear Microwave and Millimetre-Wave Circuits (INMMiC), Leuven, Belgium, April 2014, pp. 1 – 6.

[12] Y. Gurbuz, O. Esame, I. Tekin, W. P. Kang, J. L. Davidson: Diamond Semiconductor Technology for RF Device Applications, Solid-State Electronics, Vol. 49, No. 7, July 2005, pp. 1055 – 1070.

[13] M. Mohr, A. Caron, P. Herbeck-Engel, R. Bennewitz, P. Gluche, K. Brühne, H.- J. Fecht: Young's Modulus, Fracture Strength, and Poisson's Ratio of Nanocrystalline Diamond Films, Journal of Applied Physics, Vol. 116, No. 12, October 2014, pp. 1 – 9.

[14] H. J. Roper, R. E. F. Weaver, J. H. Brandon: The Effect of Peak Count of Surface Roughness on Coating Performance, JPCL- The Journal of Protective Coatings & Linings, June 2005, pp. 52 – 64.